UNIVERSITAT POLITÈCNICA DE VALÈNCIA

UNIVERSITAT POLITÈCNICA DE VALÈNCIA

Escuela Técnica Superior de Ingeniería Industrial

Powertrain dimensioning for a self-propelled freight wagon

Trabajo Fin de Grado

Grado en Ingeniería en Tecnologías Industriales—Grau en Enginyeria en Tecnologies Industrials

AUTOR: Santana Gimeno, Héctor

Tutores: Sancho Vivó, Salvador; Palsson, Björn

CURSO ACADÉMICO: 2023/2024

CHALMERS

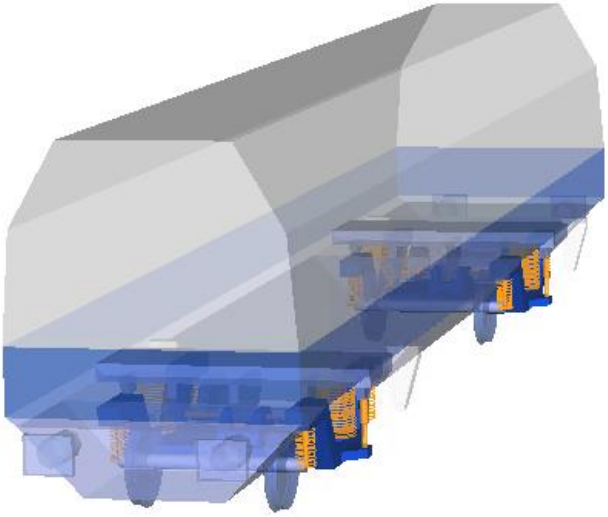

Powertrain dimensioning for a self-propelled freight wagon

Bachelor's Thesis in the Bachelor's Degree in Industrial Engineering

HÉCTOR SANTANA GIMENO

Department of Mechanics and Maritime Sciences
Division of Dynamics
Railway Mechanics
CHALMERS UNIVERSITY OF TECHNOLOGY
Göteborg, Sweden 2024

BACHELOR'S THESIS IN INDUSTRIAL ENGINEERING

Powertrain dimensioning for a self-propelled freight wagon

HÉCTOR SANTANA GIMENO

Department of Mechanics and Maritime Sciencies
Division of Dynamics
Railway Mechanics
CHALMERS UNIVERSITY OF TECHNOLOGY
Göteborg, Sweden 2024

Powertrain dimensioning for a self-propelled freight wagon

HÉCTOR SANTANA GIMENO

ISSN 1652-8557
Department of Mechanics and Maritime Sciences
Division of Dynamics
Railway Mechanics
Chalmers University of Technology
SE-412 96 Göteborg
Sweden
Telephone: + 46 (0)31-772 1000

Department of Mechanics and Maritime Sciences
Göteborg, Sweden 2024

Powertrain dimensioning for a self-propelled freight wagon

Master's Thesis in the Bachelor's Degree in Industrial Engineering

HÉCTOR SANTANA GIMENO
Department of Mechanics and Maritime Sciences
Division of Dynamics
Railway Mechanics
Chalmers University of Technology

ABSTRACT

The mobility industry has evolved rapidly in recent years with the objective of reducing emissions through electrification and efficiency improvements. The European Union is strongly committed to supporting this change with various programs involving all types of vehicles. TRANS4M-R is one of these projects, focused on transforming the rail freight sector in Europe to make it more sustainable, efficient, and automated. To help achieve these goals, this thesis aims to verify the viability of adding a self-propulsion system to the wagons for autonomous operation. To meet this objective, the electric propulsion system has been dimensioned through a series of simulations of a freight wagon in different use cases, focusing on curving resistance, track design, energy consumption, and required power. This report covers the design, simulation, and results discussion of a standard freight wagon on example tracks, along with a brief description of the current state of this new technology.

Key words: Dimensioning, Freight wagons, Innovation, Viability, Railway vehicles, Simulation, Batteries, Electric mobility

Contents

List of figures

List of tables

Notations

D_A	Aerodynamic resistance force [N]
D_R	Rolling resistance force [N]
C_D	Drag coefficient [-]
C_o	Coefficient aerodynamic phenomena in inter-car gaps [kg/(ms)]
C_P	Pressure coefficient [-]
C_L	Length coefficient [m^{-1}]
ρ	Air density [$\mathrm{kg/m}^3$]
A	Cross-sectional area of the wagon [m^2]
v	Vehicle speed [m/s]
q	Ventilation flow [kg/s]
L_T	Length of the wagon [m]
a_r	Starting resistance [-]
a_Q	Track condition coefficient one [-]
b_Q	Track condition coefficient two [s/m]
Q_i	Axle load [N]
F	Tractive force [N]
α	Available adhesion [-]
g	Acceleration of gravity [$\mathrm{m/s}^2$]
m_α	Weight on the axle [kg]
τ	Drive torque [Nm]
r	Wheel radius [m]

a_l	Lateral acceleration [m/s^2]
R	Curve radius [m]
σ_{cr}	Curving resistance coefficient [N/kN]
a	Constant curving resistance one [Nm/kN]
b	Constant curving resistance two [m]
c	Constant curving resistance three [Nm/kN]
d	Constant curving resistance four [m]
F_{cr}	Curve resistance force [N]
m	Weight of the entire wagon [kg]
ω	Angular velocity of the wagon [rad/s]
P	Tractive power [W]
E	Consumed energy [J]
t_o	Time of the start of the simulation [s]
t_f	Time of the end of the simulation [s]
P_r	Maximum tractive power required [W]
η_e	Efficiency of electric traction vehicle [-]
E_r	Capacity required for the battery [J]

1 Introduction

TRANS4M-R is a project of the Europe's Rail Joint Undertaking and part of the EU Horizon Europe research and innovation program. The main objective of this project is to transform the rail freight sector in Europe into a more sustainable, efficient, and automated system to accomplish a low-emission logistics chain around all Europe [1].

The project has three main objectives that can be summarized in higher efficiency and shorter transportation duration, increase flexibility and reliability of rail freight services, and improve the problems derived from the demographic change creating and applying the tools required for it [2]. The aim of this thesis is to help achieve some of these objectives by supporting the development of a self-propelled freight wagon to perform last mile delivery tasks operating autonomously. To accomplish this, a series of simulations have been made to verify the viability of adding a self-propulsion system to the freight wagons.

There is an enormous number of different freight wagons on circulation around Europe, so as the idea of this thesis is to give an initial dimensioning of a general self-propelled freight wagon to see its viability, standard values have been used in terms of coefficients in formulas and lengths in the model. If the idea is to apply a real dimensioning to a specific freight wagon to make it self-propelled, some changes should be done to the simulation model to adapt it to that specific freight wagon.

2 Vehicle requirements

The objective of this thesis is to dimension a self-propelled freight wagon capable of traveling short distances at relatively low speeds. Consequently, the requirements outlined in Table 2.1 ensure an appropriate use case scenario. These considerations were rigorously examined during the simulations to verify the correct functioning of the freight wagon even in the worst-case scenario.

Requirements	
Average velocity	$20\ \mathrm{km/h}$
Maximum traction force	$16\ \mathrm{kN}$
Maximum lateral acceleration	$1\ \mathrm{m/s^2}$
Maximum track length	$10\ \mathrm{km}$
Maximum track gradient	1.5%
Minimum curve radius	$100\ \mathrm{m}$

Table 2.1: Requirements considered for the freight wagon.

3 Benchmarking

The idea of creating a self-propelled wagon is relatively new, and because of that there are not so many options in the market. Currently most of them are ideas and prototypes, but they are also interesting and will be commented in this section of the thesis.

3.1 Intramotev

Probably the most interesting one, because it is the only one that has been implemented in a real case scenario, is "ReVolt", a self-propelled battery freight car developed by an American company named Intramotev. This vehicle uses regenerative braking and batteries to reduce the locomotive's fuel consumption and it has been deployed on a mining railway in Pennsylvania, as part of a standard freight train visible in Figure 3.1. Today it has covered more than 1600 km on a 27 km isolated line. [3][4]

Figure 3.1: Intramotev's self-propelled freight car in a standard freight train. [3]

3.2 RZV Čakovec

RZV Čakovec and partners have developed a prototype of a self-propelled wagon with a 55 kW diesel generator and a maximum velocity of 100 km/h to move around worksites under remote control (Figure 3.2). Their intention is that a locomotive would bring the wagons to a worksite and then uncouple them and return to base. After this the wagons would be able to move around the site and to nearby worksites by their own. Also, there is the option of use them to move freight with a range of 1 km. For now, nothing is known about future development or use of the prototype. [5]

Figure 3.2: The RZV Čakovec self-propelled freight wagon on display at the InnoTrans in 2014. [5]

3.3 Parallel Systems

An interesting approach is the concept under development by Parallel Systems, a start up from California created by former SpaceX Engineers. It consists of independent mobile drive units or carriers, in the format of traditional bogies, that can carry normal intermodal containers as shown in Figure 3.3. These electric carriers are self-sufficient and autonomous, so they have their own energy supply, traction and braking systems. A pair of carriers can carry up to 58000 kg, cover 800 km between charges, and recharge in less than an hour. They also feature camera-based perception systems. [6][7]

Figure 3.3: Parallel Systems' electric carriers carrying containers. [6]

3.4 Henan

Henan is a manufacturing company with many patented technologies, including freight wagons. Their products are focused on applications inside plants as shown in Figure 3.4, but their main selling point is the modular design of their products, making them highly customizable and easily adaptable to any kind of plant. [8]

Figure 3.4: Henan's RGV Intelligent Rail Transfer Cart. [8]

4 Model presentation

For the execution of this project, a passenger vehicle model created in Simpack from [9] was used as a starting point. This model was then adapted to function as a self-propelled freight car.

4.1 Vehicle model

The simulated freight wagon is a rigid body dynamics model including a car body and two bogies, each with two wheelsets. Given the low speed and power requirements for the self-propelled wagon, only one of the four wheelsets provides torque to achieve maximum simplicity and this is sufficient to provide the necessary tractive power. Figures 4.1 – 4.3 provide a visualization of the freight wagon.

Given the wide variety of freight cars currently in existence, the aim was to create a model with standard dimensions and weight [10], which are detailed below:

- The body measures 16.59 meters in length, 4.05 meters in height (0.5 meters above the ground) and its widest section is 3.02 meters. Its weight is 72000 kg.
- The bogies are spaced 10 meters apart from their respective anchor points. Each bogie weighs 2615 kg.
- The two wheelsets of each bogie are 2.56 meters apart, and their wheels have a radius of 0.46 meters. Each wheelset weighs 1813 kg.

Figure 4.1: Side view of the freight wagon.

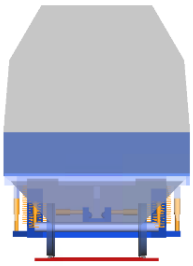

Figure 4.2: Front view of the freight wagon.

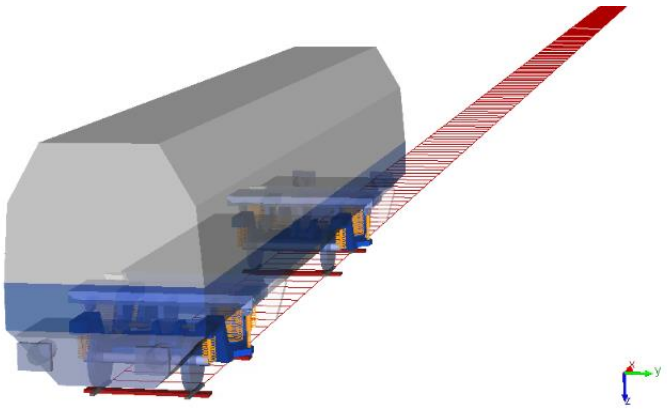

Figure 4.3: General view of the freight wagon.

Suspension stiffness was doubled compared to the original model. Additionally, to account for different stiffnesses in the freight wagons, a yaw stiffness factor is applied. This factor multiplies all stiffnesses in the primary and secondary suspension related to yaw to determine the variation in curving resistance. For the dimensioning of the freight wagon, the yaw stiffness factor is set to 2.

4.2 Resistance force modelling

Two external resistance forces, aerodynamic resistance and rolling resistance, have been added to the simulation model as they are not accounted for in the base model. To apply both resistances, two force elements have been created and applied to the model, which follow the formulas from [10]:

$$D_A \approx \frac{1}{2}\rho \cdot A \cdot C_D \cdot v^2 + (q + C_o \cdot L_T) \cdot v \tag{4.1}$$

$$C_D = C_P + C_L \cdot L_T \tag{4.2}$$

$$D_R \approx a_r \cdot \sum_{i=1}^{n_{ax}} (65 + a_Q \cdot Q_i) + \sum_{i=1}^{n_{ax}} (b_Q \cdot Q_i) \cdot v \tag{4.3}$$

In the formula for aerodynamic resistance (Equation 4.1), ρ is the air density (1.3 kg/m^3), A is the cross-sectional area of the wagon (9.3695 m^2), C_D is the drag coefficient, v is the speed of the wagon, q is the ventilation flow (0 kg/s as the wagon is considered completely closed), C_o is a coefficient dependent on the aerodynamic phenomenon related to the inter-car gaps (0 kg/(ms)) as the inter-car gaps are not considered), and L_T is the length of the wagon (16.59 m). The drag coefficient (C_D) has been calculated using Equation 4.2, in which C_P is the pressure coefficient (0.7) and C_L is the length coefficient (0.007 m^{-1}).

To calculate the rolling resistance, Equation 4.3 has been used, where a is the starting resistance (1 as the simulation starts with the wagon running), Q_i is the load on axle i (207.1921 kN), and finally a_Q and b_Q are coefficients dependent on the condition of the track ($0.75 \cdot 10^{-3}$ and $1 \cdot 10^{-5}$ s/m).

4.3 Limitations Applied to the Model

As mentioned in the requirements, the freight wagon has been simulated with a maximum traction force of 16 kN. This consideration is based on freight train examples in [10], where a typical electric freight train can provide around 200 N per ton. Also, it respects the restriction related to adhesion presented in [11]:

$$F \leq \alpha \cdot g \cdot m_\alpha \tag{4.4}$$

In Equation 4.4 α is the available adhesion and was considered 0.2 according to [10], because the velocity is always under 50 km/h and the slip control will probably be simple, g is the acceleration of gravity equal to 9.81 $\mathrm{m/s^2}$ and m_α is the weight (mass) on the axle considered 21.1205 t, resulting in a maximum tractive force F of 41.44 kN that is considerably bigger than the limit established ensuring that the utilized adhesion is smaller than the available adhesion. To apply this limitation to the model the maximum torque that the axle can provide has been limited:

$$\tau = F \cdot r \tag{4.5}$$

To calculate the maximum torque, Equation 4.5 has been used, where F is the maximum force and r is the wheel radius (0.46 m), resulting in a torque of 7.360 kN·m. This maximum torque also limits the maximum velocity the freight wagon can reach in each part of the track, so the constant speed of 20 km/h considered is maintained only if the torque required is less than the maximum calculated.

5 Simulated tracks

For this project, two tracks with different operating modes have been simulated to extract different data of interest to dimension the powertrain.

5.1 Progressively decreasing curve radius

As its name indicates, this track consists of a curve with a progressively decreasing radius, starting at 500 m, and ending at 100 m (Figure 5.1 and 5.2). To simulate it, the lateral acceleration has been set to 1 $\mathrm{m/s^2}$ during the entire curve with a speed controller, which is the limit considered for this wagon. To calculate the speed during the simulation, Equation 5.1 has been used, where a_l is the lateral acceleration (1 $\mathrm{m/s^2}$) and R is the radius of the curve.

$$v = \sqrt{a_l \cdot R} \tag{5.1}$$

Figure 5.2 shows that the track is divided into two types of sections: constant radius curves and transition zones. The transition zones, which consist of curves with a continuously decreasing radius, help the wagon smoothly transition between different curve radii.

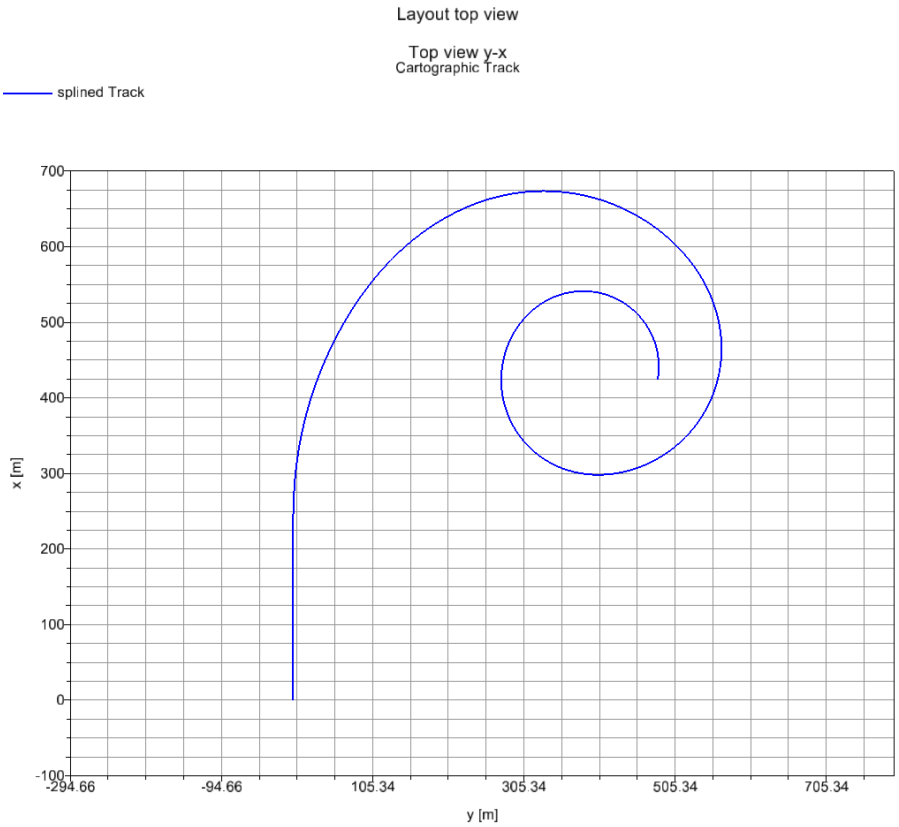

Figure 5.1: Progressively decreasing curve radius track top view.

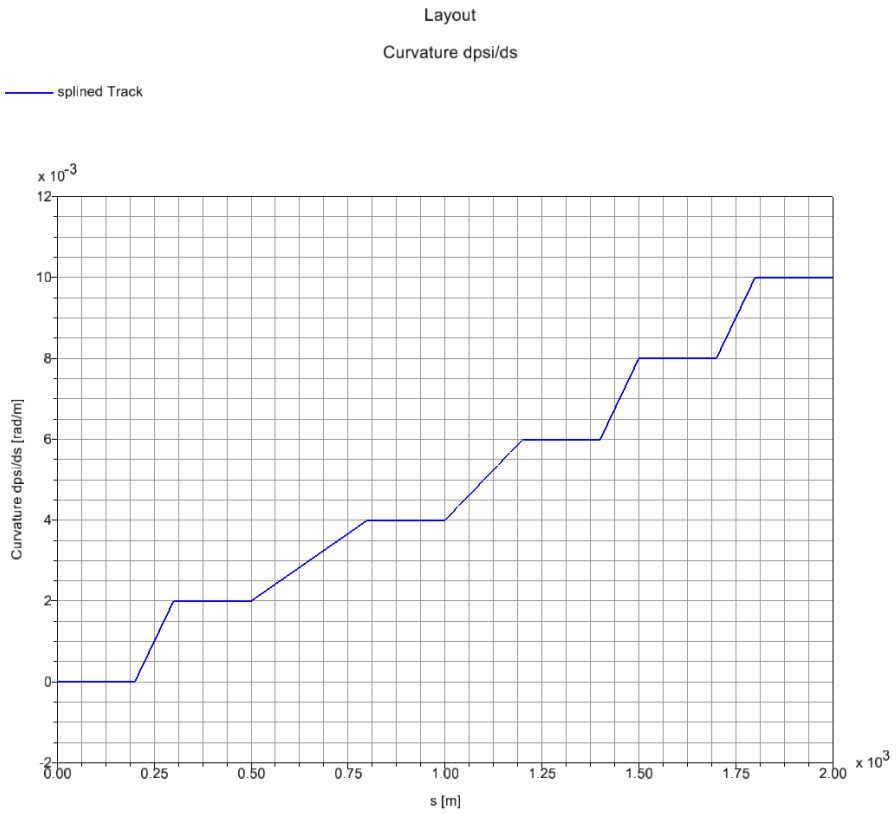

Figure 5.2: Progressively decreasing curve radius track curvature per meter of track.

5.2 10 km track with high demands

For this track, the aim was to simulate scenarios of maximum demand for the freight wagon. This includes gradients of up to 1.5%, as shown in Figure 5.4, curves with a radius as small as 100 m, visible in Figure 5.3 and 5.5, and combinations of both. The two most demanding sections are located at the end of the track, consisting of a 1.5% gradient in a curve with a 500 m radius and a 1% gradient in a curve with a 125 m radius.

The initial speed for this track is 5 km/h. After traveling 10 meters, the wagon accelerates to the required velocity of 20 km/h. Finally, before completing the track, it decelerates back to 5 km/h.

Figure 5.3: 10 km track with high demands top view.

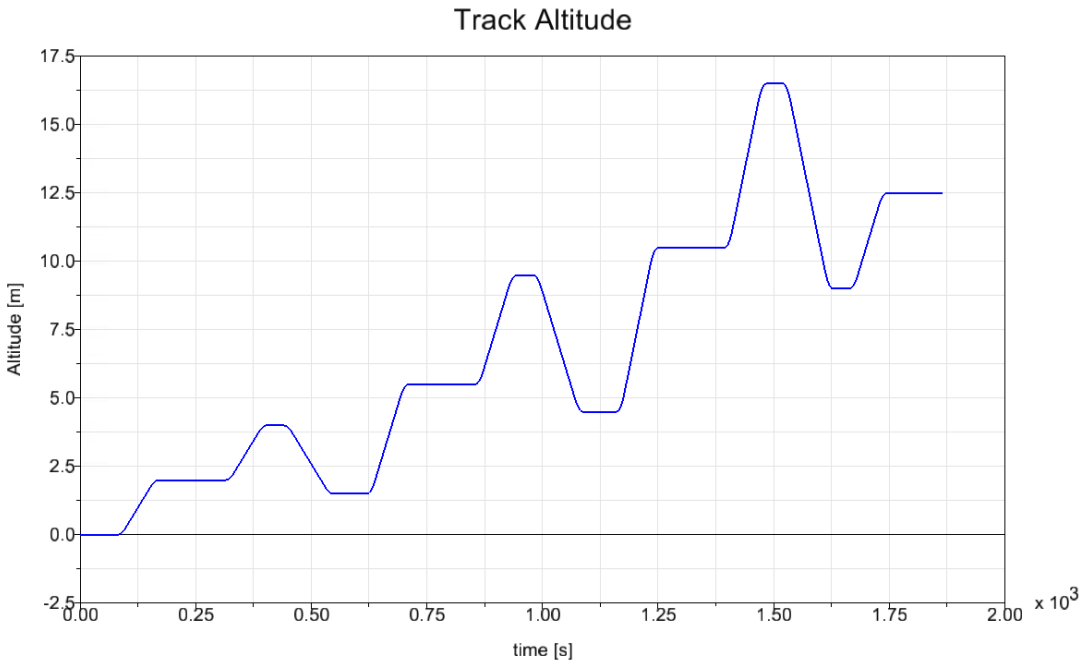

Figure 5.4: 10 km track with high demands altitude.

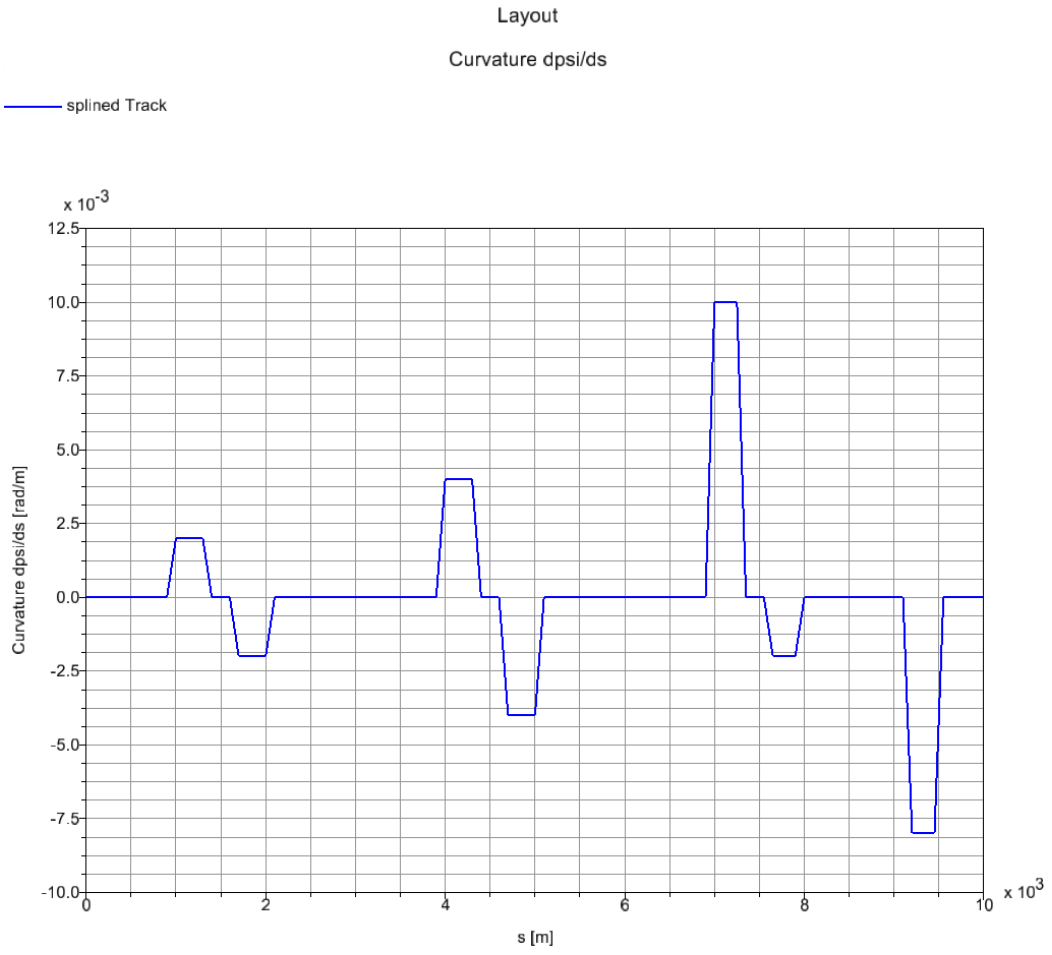

Figure 5.5: 10 km track with high demands curvature per meter of track.

6 Simulation results

In this section, the most notable results of the simulations are presented and compared to empirical formulas. Additionally, the postprocessing of the data is explained, including calculations useful for dimensioning, which will be utilized in the subsequent section. Following this, the necessary data for sizing has been extracted, and graphs of significant interest are included.

6.1 Curve resistance

After simulating the route with the progressively decreasing radius curve, we can extract the curve resistance for each radius and for the different yaw stiffnesses, as shown in

Table 6.1. The curving resistance is determined by the tractive effort needed to propel the vehicle through the curve with aerodynamic and rolling resistance forces deactivated in the model. The results of the simulation show that the curve resistance is greatly influenced by the variation of the yaw stiffness, and it increases exponentially when reducing the radius of the curve. This means that gradients with tight curves are the most critical conditions for a self-propelled wagon.

It could also be interesting to compare the results of the simulation with the empirical formulas. For this comparison, the ones from [12] have been selected:

$$\sigma_{cr} = \begin{cases} a/(R-b) & R > 300 \\ c/(R-d) & R \leq 300 \end{cases} \tag{6.1}$$

$$F_{cr} = m \cdot g \cdot \sigma_{cr} \tag{6.2}$$

In Formula 6.1, a, b, c and d are constants that can be different in each country. For this calculation the ones proposed in [12] have been selected, which are $a = 650$, $b = 55$, $c = 500$ and $d = 30$. After this, Formula 6.2 has been used to calculate the curve resistance F_{cr}, multiplying σ_{cr} by the total mass of the wagon m (84.482 t) and by the gravitational acceleration g (9.81 m/s^2).

Reference [12] states that these formulas lack precision because they do not account for velocity or superelevation. However, as shown in Figure 6.1, the values for radii above 300 m align closely with the simulation results. For radii under 300 m, the accuracy is not as high, but the formulas still provide a good approximation of the real values. The main problem with these formulas is the big difference in the 300 m radius point where there is a difference of 30%.

Yaw Stiffness	R (m)	τ (Nm)	F(N)
2	500	450	978,26
	250	1159	2519,57
	167	1938	4213,04
	125	2760	6000
	100	3539	7693,48
4	500	481	1045,65
	250	1210	2630,43
	167	2001	4350
	125	2812	6113,04
	100	3577	7776,09
6	500	493	1071,74
	250	1233	2680,43
	167	2033	4419,57
	125	2846	6186,96
	100	3623	7876,09
8	500	499	1084,78
	250	1251	2719,57
	167	2064	4486,96
	125	2885	6271,74
	100	3680	8000
10	500	503	1093,48
	250	1268	2756,52
	167	2113	4593,48
	125	2962	6439,13
	100	3769	8193,48

Table 6.1: Curve Resistance with different Radii and Yaw Stiffness.

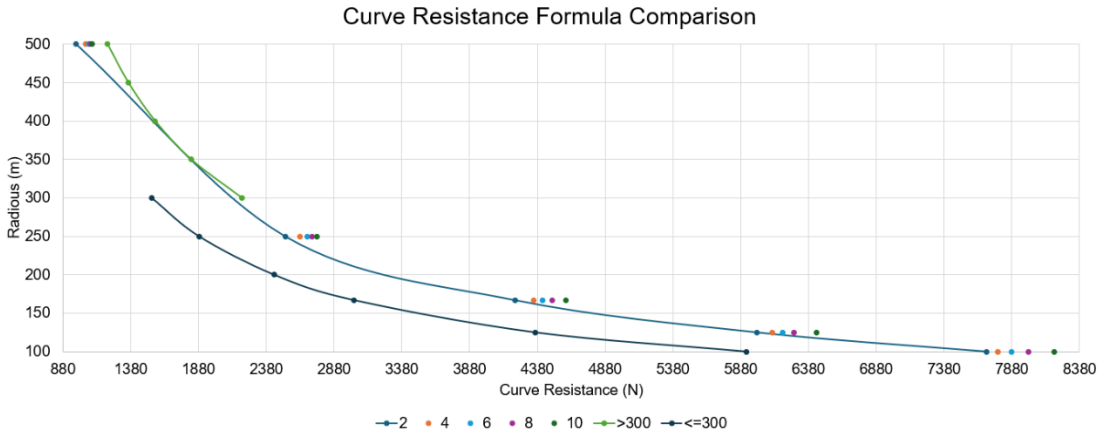

Figure 6.1: Curve Resistance Formula Comparison.

6.2 Torque

For the 10 km route, the primary interest is to extract the torque during the simulation with the aim of subsequently calculating the total consumption and the required power. Additionally, there are other data worth of mentioning. As seen in Figure 6.2, the drive torque gets higher as the track becomes more demanding. When running on horizontal track, the drive torque used corresponds to the rolling resistance and the aerodynamic drag, and comparing to the rest of the track it can be conclude that the curving and gradient resistance dominate in terms of drive torque required. The maximum torque during the simulation arrives to the limit of 7.360 kN·m. Furthermore, in Figure 6.2, the torque can be divided into two sections: the positive torque, produced by the power train, and the negative torque, produced by the brake system.

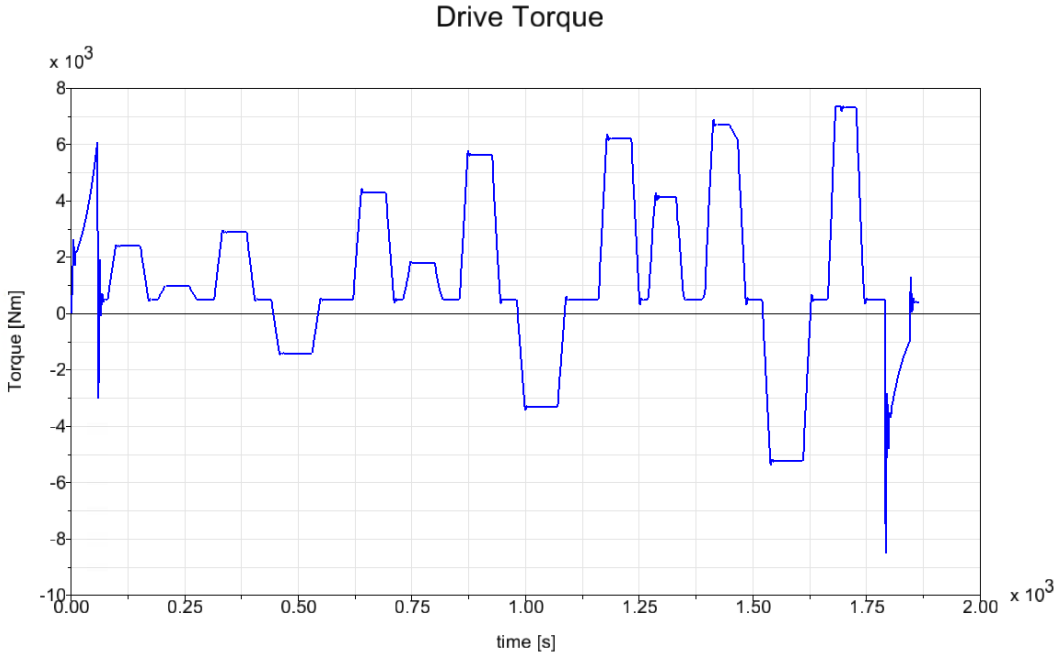

Figure 6.2: Torque on the 10 km track.

6.3 Energy consumed

To calculate the consumed energy, only the positive torque has been considered, as the brakes are an independent system. Continuing with the calculation, the following formulas have been utilized:

$$\omega = \frac{v}{r} \tag{6.3}$$

$$P = \tau \cdot \omega \tag{6.4}$$

$$E = \int_{t_o}^{t_f} P \, dt \tag{6.5}$$

With Equation 6.4, the power P is calculated by multiplying the torque by the angular velocity ω, which is determined by dividing the linear velocity by the wheel radius as shown in Equation 6.3. Finally, to calculate the consumed energy E, Equation 6.5 is used, in which the power is integrated over the simulation time, from t_o to t_f.

In Figure 6.3, the growth of the consumed energy throughout the simulation can be observed. At the end, the total consumed energy is 11.5 kWh.

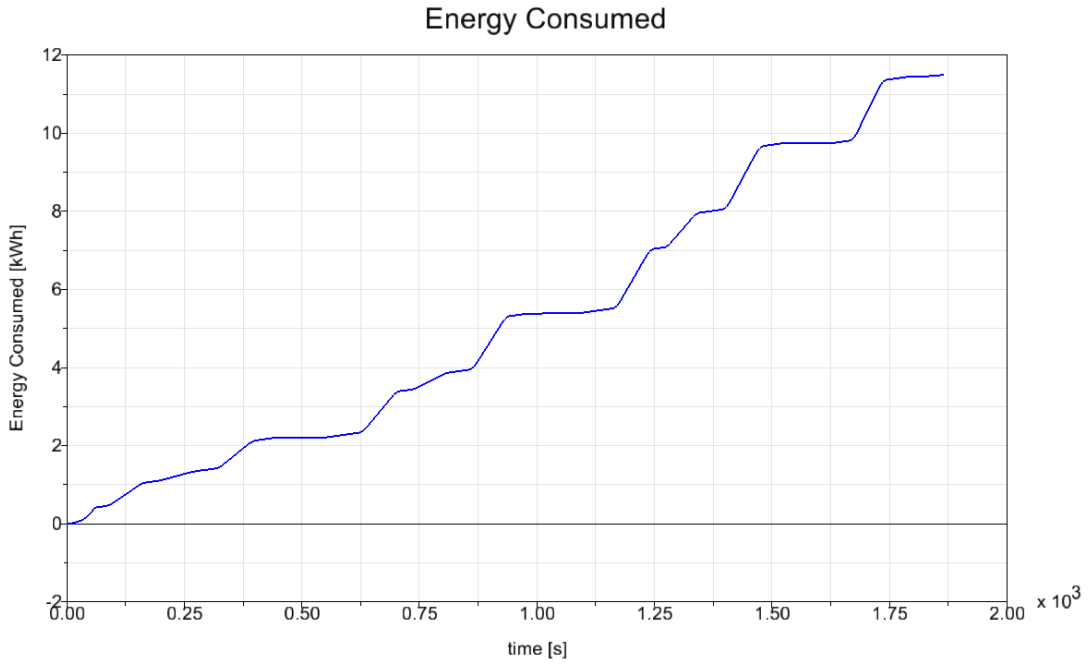

Figure 6.3: Energy Consumed without regenerative braking.

Considering regenerative braking is also interesting, as it can help reducing the overall energy consumption. The energy consumed by the braking system is determined solely by the negative torque. Figure 6.4 illustrates the evolution of the energy utilized by the braking system, indicating that up to 3.41 kWh could be potentially recovered with an ideal regenerative braking system.

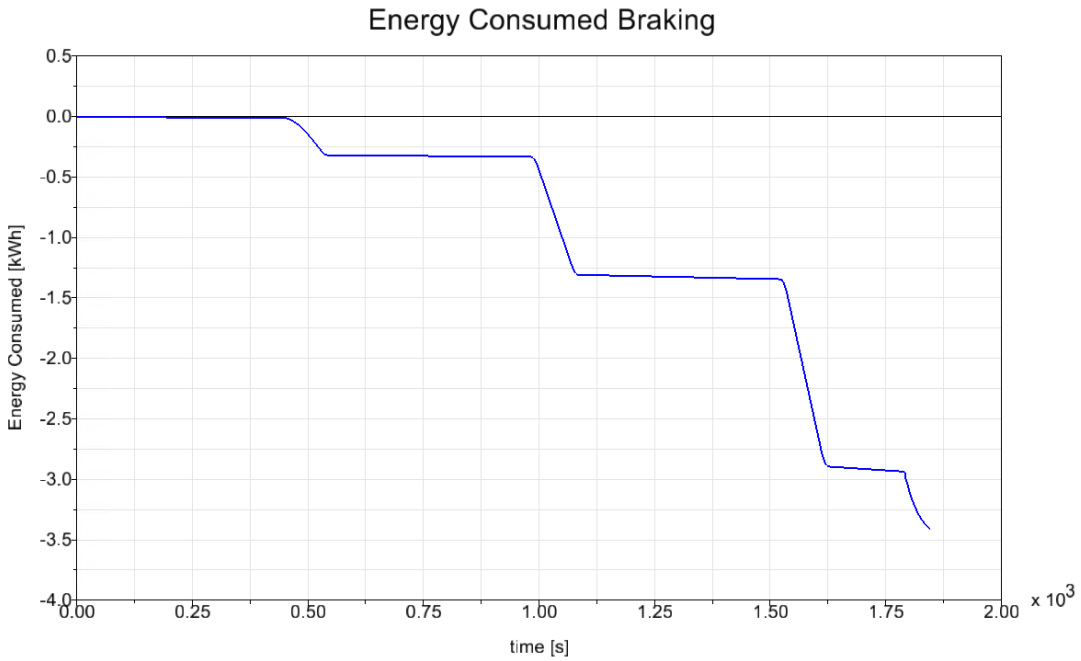

Figure 6.4: Energy Consumed for braking.

6.4 Maximum power

To determine the maximum power required, the maximum torque observed in the simulation must be identified, which is limited to 7.360 kN·m as explained earlier. Utilizing Equation 6.3 and Equation 6.4, this results in the need for a motor capable of delivering 88.89 kW to maintain a constant speed of 20 km/h.

With this power, the wagon is barely capable of surpassing the worst-case scenario on the 10 km track, which includes a curve with a radius of 125 m and a 1% gradient. This scenario must be considered the limit of the wagon's capabilities because, as observed in testing simulations, the wagon cannot complete the track if the gradient is increased to 1.5%.

7 Dimensioning

During this part of the thesis the real requirements for the incorporation of a propulsion system to the freight wagon were calculated resulting in the minimum power required as well as the minimum battery capacity needed.

7.1 Energy efficiency

Modern electric traction vehicles have high efficiency when providing a tractive force, but they still have important losses to consider. The average efficiency for this kind of vehicles is usually in the range of 80-83%. [10]

After knowing the values of efficiency ($\eta_e = 0.83$) and the maximum power used in the simulation ($P = 88.89\ kW$), the following formula has been used to obtain the real maximum power required P_r:

$$P_r = P/\eta_e \tag{7.1}$$

Using Equation 7.1 results in a maximum power required of 107.1 kW that the motor needs to be able to supply to maintain a constant speed of 20 km/h in the most demanding part of the track (curve of 125 m radius while going up a 1% slope).

7.2 Battery capacity

As the objective of the project is to create an autonomous self-propelled wagon, it is needed to incorporate a battery. To ensure a good life expectancy and efficiency, the battery charge should always be in the range of 20-80% [13][14]. Then, to calculate the total capacity required for the battery the next formula can be used:

$$E_r = E/(0.8 - 0.2) \tag{7.2}$$

In Equation 7.2, E is the total energy consumed during the simulation (11.5 kWh) and E_r the total capacity required for the battery that results in 19.17 kWh.

The value calculated before does not consider regenerative braking, which as commented previously in the thesis, is interesting to consider it too. In Figure 7.1 the evolution of energy consumption during the simulation can be observed, considering regenerative braking. In this case, when the wagon is braking, energy is transmitted to the battery, and it recharges it.

Now, for calculating the capacity needed to the battery considering regenerative braking, Equation 7.2 has also been used, but the value of energy consumed during the simulation E ($8.49\ kWh$) is the maximum value in Figure 7.1. This results in a total capacity required for the battery of 14.15 kWh with an ideal regenerative braking system. This implies that regenerative braking is an important consideration because it can reduce the battery capacity necessary by up to 25%.

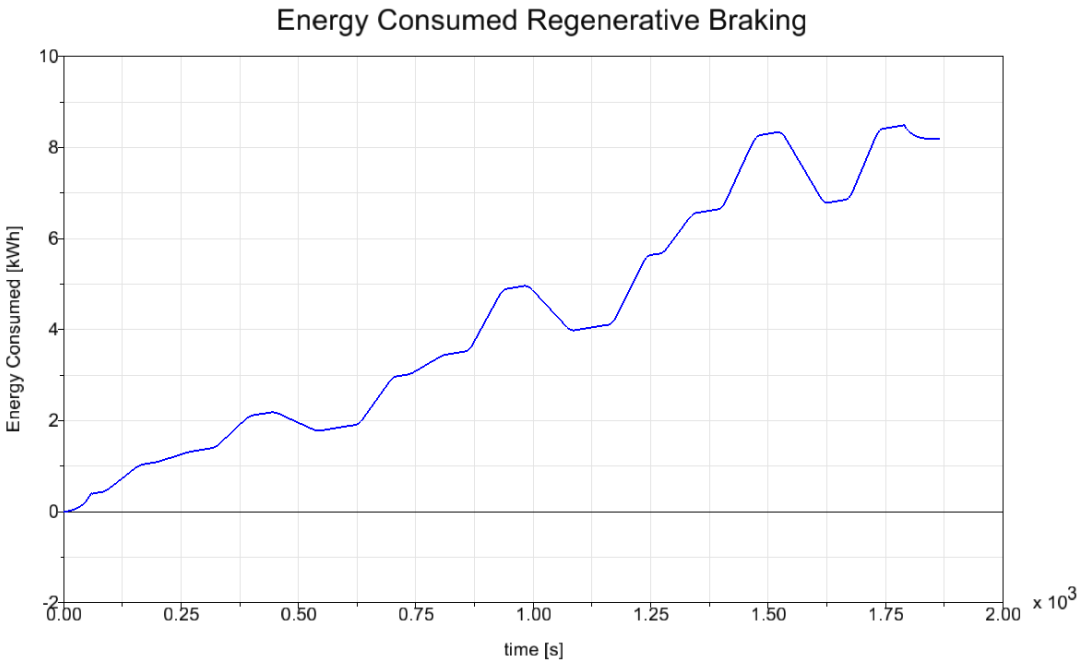

Figure 7.1: Energy Consumed considering regenerative braking.

7.3 Specific power and energy density

After calculating the required values for power and battery capacity, it is also important to evaluate them in relation to the weight of the wagon (84.482 t). The specific power, calculated as power divided by mass, amounts to 1.27 kW/t. The energy density without regenerative braking must be at least 0.227 kWh/t, and with regenerative braking considered, it should be 0.167 kWh/t.

8 Conclusions

After completing the dimensioning process, several conclusions can be drawn. Firstly, the construction of the wagon appears feasible given the requirements considered. According to [10], a typical electric freight train generally requires 2-3 kW/t of tractive power, which is significantly higher than the 1.27 kW/t calculated for the simulated wagon. Additionally, energy densities for similar distances average around 0.75 kWh/t, which is also much higher than the required energy density of 0.227 kWh/t for the simulated wagon without considering regenerative braking.

Another important aspect to highlight is the potential use of regenerative braking. Implementing regenerative braking could reduce the battery capacity needed by up to 25% in an ideal scenario. Therefore, incorporating regenerative braking into the wagon design, if feasible, should be considered. This would significantly reduce the total energy consumption, decrease the required battery capacity, enhance sustainability, and reduce both battery costs and weight.

References

[1] FP5-TRANS4M-R (2024) *Transforming Europe's Rail Freight*, https://projects.rail-research.europa.eu/eurail-fp5/, Accessed 31-05-2024

[2] FP5-TRANS4M-R (2024) *PROJECT OBJECTIVES*, https://projects.rail-research.europa.eu/eurail-fp5/objectives/, Accessed 31-05-2024

[3] Railway Gazette International (2024, April 9) *Self-propelled battery wagon deployed on mining railway*, https://www.railwaygazette.com/freight/self-propelled-battery-wagon-deployed-on-mining-railway/66263.article, Accessed 05-06-2024

[4] Intramotev (2024) *Product & Technology*, https://intramotev.com/product-technology/, Accessed 05-06-2024

[5] Railway Gazette International (2014, November 14) *Self-propelled wagon prototype*, https://www.railwaygazette.com/freight/self-propelled-wagon-prototype/40181.article, Accessed 05-06-2024

[6] Parallel Systems (2022, January 19) *Former SpaceX Engineers Raise $49.55 Million to Build Autonomous Battery-Electric Rail Vehicles*, https://moveparallel.com/wp-content/uploads/2022/01/19Jan2022_Parallel_Systems_Series_A.pdf, Accessed 05-06-2024

[7] Parallel Systems (2023, September 12) *Parallel Systems Publicly Introduces Its First Ground-Up Design with Second Generation Autonomous Battery-Electric Rail Vehicle, Setting the Path for Customer Testing on U.S. Railways*, https://moveparallel.com/wp-content/uploads/2023/12/20230912-Parallel-Systems-Mark-2-Press-Release.pdf, Accessed 05-06-2024

[8] Henan (2024) *Products*, https://www.rmk-transfercar.com/rail-transfer-car/, Accessed 05-06-2024

[9] Iwnick S. (1998) *Manchester Benchmarks for Rail Vehicle Simulation*, Vehicle System Dynamics, 30(3-4), 295-313

[10] Andersson E. et al (2018) *Rail Systems and Rail Vehicles Part 2: Rail Vehicles*

[11] Andersson E. et al (2018) *Rail Systems and Rail Vehicles Part 1: Rail Systems*

[12] Wu Q. et al (2020) *Curving resistance from wheel-rail interface*, Vehicle System Dynamics, 60(3), 1018-1036

[13] Emmanouil D. Kostopoulos et al (2020) *Real-world study for the optimal charging of electric vehicles*, Energy Reports, 6, 418-426

[14] F. Marra et al (2012) *Demand profile study of battery electric vehicle under different charging options*, 2012 IEEE Power and Energy Society General Meeting, San Diego, CA, USA

[15] United Nations (2024) *Sustainable Development Goals*, https://www.un.org/sustainabledevelopment, Accessed 12-06-2024

A Curve Resistance Plots

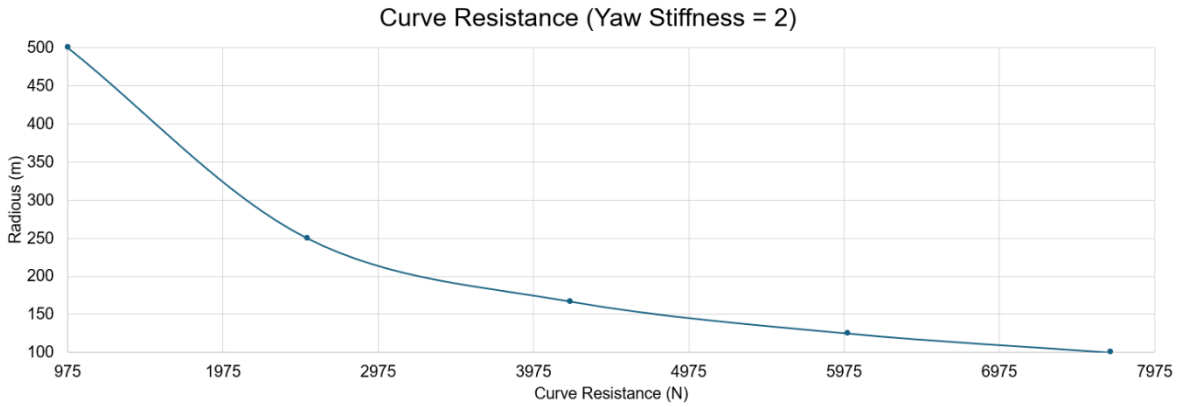

Figure A.1: Curve Resistance (Yaw Stiffness = 2).

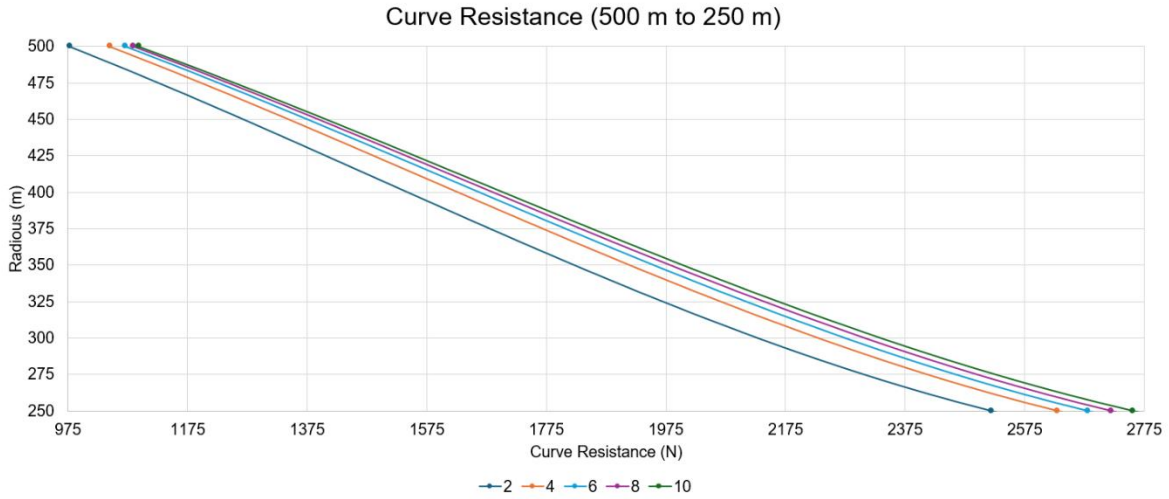

Figure A.2: Curve Resistance (500 m to 250 m).

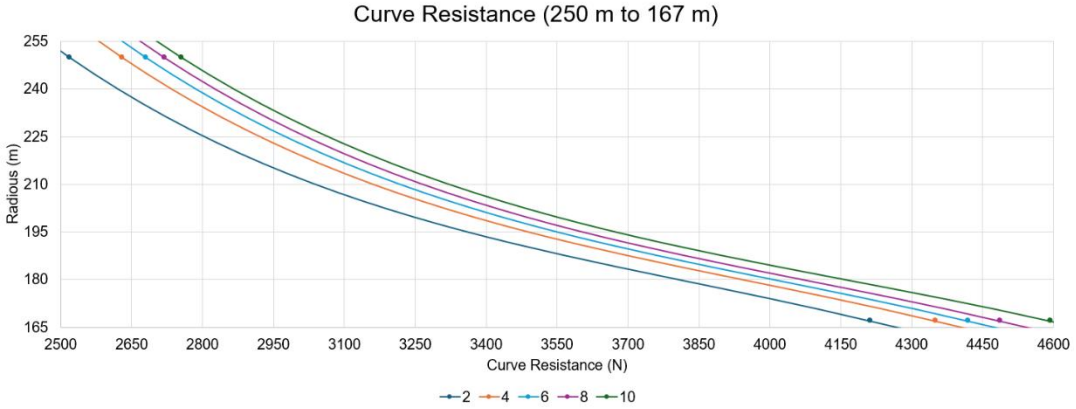

Figure A.3: Curve Resistance (250 m to 167 m).

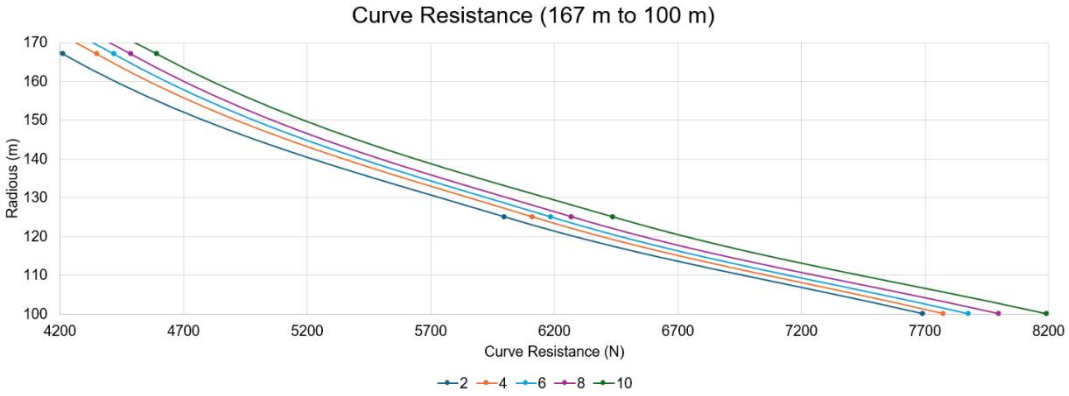

Figure A.4: Curve Resistance (167 m to 100 m).

B Sustainable Development Goals

Figure B.1: Relation of the Thesis with the Sustainable Development Goals of the 2030 Agenda. [15]

"The content of this publication has not been approved by the United Nations and does not reflect the views of the United Nations or its officials or Member States."